Prepared By : Neill Tucker	No. 08:002		
Project Title : Array Design Toolbox for MATLAB	Date 15/06/09	Rev D	File C:\ My Documents \ Array Design\ ArrayCalc10d.doc

Phased Array Design Toolbox V2.4

for MATLAB

Theory of Operation

by N. Tucker

ABSTRACT

In recent years the advances in computer technology has led to increasing use of numerical techniques in the design and development of antennas and related technology. Of particular prevalence are full wave microwave solvers, used to obtain the current densities on and thereby radiated fields for arbitrary structures. However, despite the increases in computer power, array antennas can be electrically very large and therefore still represent a significant analysis problem. As the number of elements in the antenna array increases, its radiated characteristics tend to be dominated by the geometric layout and excitation of the component elements, rather than the elements themselves.

Using simple mathematical models for the element radiation patterns, combined geometrically in the far field, the performance of large arrays can be calculated with reasonable accuracy for significantly less computational effort. A Matlab toolbox has been developed to enable rapid definition and analysis of 2D and 3D antenna arrays, comprising array elements such as dipole, microstrip patch, helix or any user defined element pattern function. This paper documents the theory used in the toolbox.

Prepared By : Neill Tucker	No. 08:002		
Project Title : Array Design Toolbox for MATLAB	Date 15/06/09	Rev D	File C:\ My Documents \ Array Design\ ArrayCalc10d.doc

CONTENTS

1. INTRODUCTION

Phased array antennas can be found in a wide variety of applications including communications, radar, remote sensing and biomedical. The term generally refers to a collection of radiating sources with a controllable phase (and usually amplitude) relationship with respect to each other.

From basic physics we know that 2 or more sources of sinusoidal waves, with a defined phase relationship, will generate an interference pattern. To produce the interference pattern you simply need to choose a line or surface at some distant location from the sources, the summing plane. Where the waves arrive in phase there will be reinforcement and a maxima, and where they arrive in anti-phase there will be cancellation and a minima. This summing of sine waves according to relative distance (and therefore phase) between the source and points on the summing plane, is really all that is required to calculate the radiation pattern of a phased array. The difficulty tends to arise when the sources are directional and located in 3 dimensions, the summing process is identical, it just makes the trigonometry more challenging.

In my first job in antenna design, my mentor gave me some very sound advice “if you want to be a good antenna engineer, get your head around 3D coordinate geometry”. Indeed, many of the derivations we take for granted, such as the radiation pattern of a dipole, owe as much to trigonometry as to electromagnetic theory.

To understand how this geometric approach to array design fits in with “true” electromagnetic modelling, a quick look at how full-wave solvers deal with the problem may be helpful. Design packages such as HFSS, IE3D, Sonnet and NEC all use the same basic method.

1) Divide the structure into small segments.

2) Assign a function (basis function) to each segment, representing the current density on it.

3) Generate a matrix equation that represents the inter-action between each segment and every other.

4) Solve the interaction-matrix equation, usually by inverting it, to get coefficient values for the basis functions and thereby the current densities.

5) Calculate the far-field patterns and other parameters using the currents on each segment.

Although this is a simplified description of the algorithm it illustrates that the number of segments involved can grow very quickly. The phrase “between each segment and every other” in step3 indicates that the computational problem is proportional to N^2, where N is the number of segments. For example, as a general rule segments should not have dimensions greater than 1/10th of a wavelength, so a single half-wave microstrip patch will require at least 5x5=25 segments. An 8x8 array of patches results in 1600 segments and therefore a 1600x1600 matrix to invert, not a trivial problem even with today's hardware. The benefit of the full wave solution is that just about all the parameters of interest can be derived from the current densities, once calculated. These parameters include far-field patterns, near-fields, input impedance and mutual coupling. The down side is that the bulk of the computational effort is in solving the matrix equation and this must be done to find one or all of the parameters listed. Although the geometrical approach yields only pattern information, the advantage is that the computational effort is related directly to the amount of information required, with little or no redundant calculation.

In later stages of the design process it is certainly important to be able to calculate parameters such as input impedance, coupling and near fields, and it is worth the extra effort. However, the usual reason for employing a phased array antenna is to produce a specific array pattern, with beam widths, side-lobe levels, null positions and directivity being of particular interest. These parameters are readily calculated using the geometric method proposed here.

Also, the full-wave solver requires a complete description of the physical structure, including feed port definitions for every active element. Despite dramatic improvements in the front-end geometry editors, changes in element size, spacing and excitations are likely to involve a lot of typing and mouse clicking. In the geometric approach, a tokenised description of the array geometry (element orientation, position excitation and element type) is used and can be edited very easily using simple command scripts.

To achieve the desired array pattern the modelling process can be used in two ways :

Pattern simulation, where an array is designed using established rules governing element spacing and amplitude/phase distributions, modelling software is used to verify and fine tune the design.

Pattern synthesis, where a desired array pattern is specified using a template, suitable amplitude/phase excitations are then searched for to give the desired pattern. Depending on the required pattern, the array excitations may not be immediately obvious, so an optimisation loop is usually required.

In the first method it is advantageous to be able to construct the array geometry easily so trade-offs between different configurations can be evaluated quickly. In the second method the rapid evaluation of the array pattern is essential since the optimisation may require many iterations to converge.

Bearing in mind these requirements and previous comments, it is felt that the geometric approach can offer some advantages for the initial stages of phased array design. It allows a basic analysis of structures that are too large for a complete full wave solution. Also because of the idealised analysis (no impedance or mutual coupling is taken into account) it can be useful in providing a benchmark for the design, allowing the designer to separate out the performance due to the fundamental geometry and excitation from other more subtle effects.

2. COORDINATE SYSTEMS AND TRANSFORMS

Before going into detail about the modelling of array elements themselves, it may be useful to look at the coordinate systems, transforms and terminology that are used.

2.1 Global Coordinate System

First there is the global coordinate system definition, shown in figure 2.1-1 in both spherical and cartesian forms. This is fairly standard in antenna textbooks but contrary to most maths texts where theta and phi are the other way around. The equations inset are used to swap between the two systems, the atan2 function is a 4-quadrant arc-tangent valid over the range –pi to +pi.

<u>Basic cartesian/spherical coordinate transforms</u>

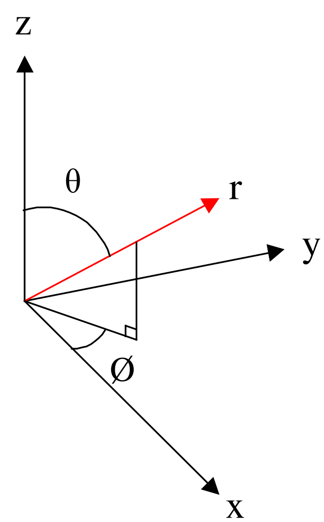

Spherical to Cartesian

$$x = r\cos(\varnothing)\sin(\theta)$$
$$y = r\sin(\varnothing)\sin(\theta)$$
$$z = r\cos(\theta)$$

Cartesian to Spherical

$$r = \mathrm{sqrt}(x^2 + y^2 + z^2)$$
$$\theta = \mathrm{acos}(z/r)$$
$$\varnothing = \mathrm{atan2}(y/x)$$

Fig 2.1-1 Global Coordinate System and Transforms

When this coordinate system is used in the context of antenna modelling or measurement there are few terms and definitions that are helpful :

Mechanical bore-sight	The intended direction of maximum radiation referenced to the antenna's mechanical structure.
Electrical bore-sight	The actual direction of maximum radiation.
Main beam	Refers to the lobe of the antenna pattern containing the most radiated energy, usually centred on the electrical bore-sight.
Beam squint	The difference between mechanical and electrical bore-sight directions, normally regarded as an error in non-array type antennas.
Beam scanning	Progressive squinting of the electrical bore-sight.

For planar array antennas the mechanical bore-sight is usually the direction normal to the physical plane of the antenna. The electrical bore-sight is the direction of maximum radiation when the relative phase and amplitude of all elements is equal. The antenna can be squinted off the bore-sight by appropriate choice of phase and amplitude distribution across the array.

For modelling purposes it is convenient to align the antenna's mechanical bore-sight with the Z-axis. A full sphere of pattern data can then be obtained by sweeping theta from -pi to pi for selected values of phi from 0 to pi. This is referred to as taking "theta cuts", sweeping phi for selected theta values is unsurprisingly termed "phi cuts". This arrangement means the when the array is squinted off bore-sight, the squint by definition will be in the plane of a theta-cut, making it is easy to plot. Plotting patterns in the plane in which squint has been applied is important for reasons that will be clear when you see what happens to the side lobe levels.

Note that for practical measurement purposes the antenna's mechanical bore-sight is usually aligned with the X-axis. This is so the Azimuth and Elevation of an AZ over EL positioner correspond directly to phi and theta respectively. Care should therefore be taken when using measured data in the 'interp' element model (ref section 5.6).

2.2 Local Coordinate System

The global coordinate system has been established as a reference for the antenna array as a whole, the array however, is made up from individual "elements". Each of these elements can be considered as an antenna in its own right and for modelling purposes it is useful to assign each element its own local coordinate system. As far as the element is concerned the local system is identical to the global system.

To create an array, elements (represented by their local coordinate systems) can be placed in specific locations and orientations in the global system. This is accomplished by using a 3D rotation matrix and offset vector. The rotation matrices in figure2.2-1 define rotations about each of the orthogonal X,Y and Z axes.

<u>Rotation matrices for successive rotations around an orthogonal axis set</u>

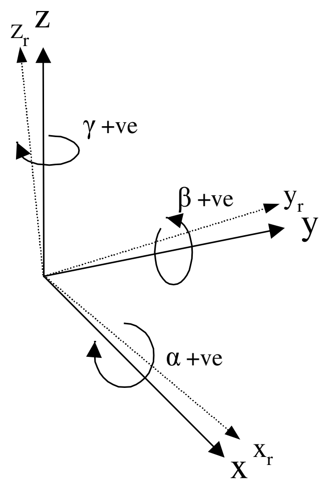

Rotation	*Matrix*	*Denoted by*
Rotation α about x-axis	$\begin{matrix} 1 & 0 & 0 \\ 0 & \cos(\alpha) & \sin(\alpha) \\ 0 & -\sin(\alpha) & \cos(\alpha) \end{matrix}$	**[XR]**
Rotation β about y-axis	$\begin{matrix} \cos(\beta) & 0 & -\sin(\beta) \\ 0 & 1 & 0 \\ \sin(\beta) & 0 & \cos(\beta) \end{matrix}$	**[YR]**
Rotation γ about z-axis	$\begin{matrix} \cos(\gamma) & \sin(\gamma) & 0 \\ -\sin(\gamma) & \cos(\gamma) & 0 \\ 0 & 0 & 1 \end{matrix}$	**[ZR]**

Figure 2.2-1 3D Roatation Matrix Definitions

These matrices can be used in isolation or combined to form a transform matrix linking points in the fixed axis set (X,Y,Z), to the rotated axis set (Xr, Yr, Zr). The 3x3 transform matrix is denoted by [T], the offset matrix by [Toff] and point coordinates in (X Y Z) and (Xr Yr Zr) are denoted by [A] and [Ar] respectively.

$$\underset{[T]}{\begin{matrix} L & M & N \\ O & P & Q \\ R & S & T \end{matrix}} * \underset{[A]}{\begin{matrix} X \\ Y \\ Z \end{matrix}} + \underset{[Toff]}{\begin{matrix} Xoff \\ Yoff \\ Zoff \end{matrix}} = \underset{[Ar]}{\begin{matrix} Xr \\ Yr \\ Zr \end{matrix}} \qquad \text{Eq 2.2-1}$$

Coordinates can be transformed in the reverse direction using the relation :

$$\mathbf{[A] = [T]^{-1} * ([Ar] - [Toff])} \qquad \text{Eq 2.2-2}$$

To construct the transform matrix, three successive rotations can be combined in the following manner:

[T] = [ZR] * [YR] *[XR]

Note that the rotations are successive. Having rotated the axes about the Z-axis using [ZR], the Y-rotation will be around the new Y-axis. Similarly the X-rotation [XR] will be around the already twice rotated new X-axis. This of course means that the order of rotation is important :

[ZR]*[YR]*[XR] ≠ [XR]*[YR]*[ZR]

Array Pattern Calculation Geometry

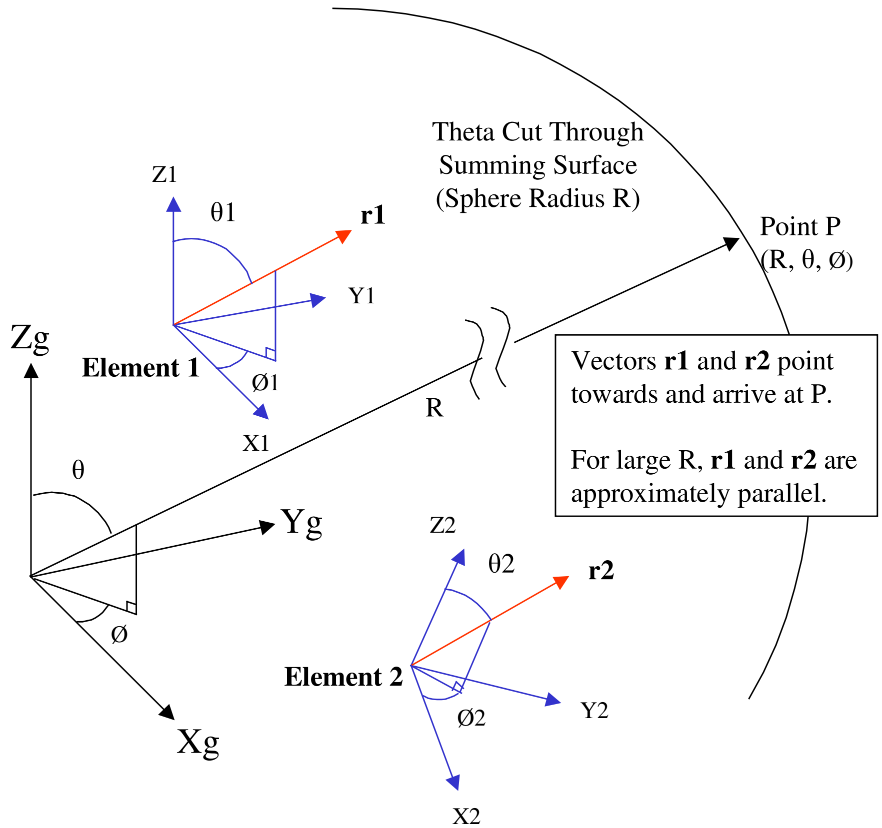

Figure 2.2-2 Array Geometry

To see how all this coordinate juggling might be helpful in analysing an array antenna, an example 2 element array is illustrated in figure2.2-2. The 2 elements are located in the global coordinate system together with a point P located on a sphere radius R. If element 1 has the transform and offset matrix [T1] & [Toff1] then point Ps location in local coordinates is given by using [T1] & [Toff1] in equation 2.2-2. Local cartesian coordinates can then be converted to spherical form to give Ps location in local (r_1,$theta_1$,phi_1). The same procedure can of course be applied to element 2 using its transform and offset matrices.

Since the radiation patterns for many small antennas such as patches, dipole and helix can be readily characterised over (r,theta,phi) using simple formula, we now have means to calculate the contribution of each element at the point P. By summing the contributions for all array elements and moving P to describe theta or phi cuts, antenna patterns can be produced. The calculations can be summarised by equation 2.2-3.

Array Pattern Summation Equation

$$\boxed{E_{tot}(\theta,\phi) = \sum_{n=1}^{N} A_n F_n(\theta_n,\phi_n) e^{-j(ko|r_n|+\beta_n)}} \qquad \text{Eq 2.2-3}$$

$E_{tot}(\theta,\phi)$ Total E-field at point P in linear volts for N elements

$F_n(\theta_n,\phi_n)$ Element pattern function for (n)th element in linear form, un-normalised and unitless

A_n Amplitude of element (n) in linear volts

$|r_n|$ Distance from element (n) to point P in meters

$ko = \dfrac{2\pi}{\lambda_0}$ Propagation constant in radians/meter

β_n Phase of element (n) in radians

Equation 2.2-3 The Summation Equation

As you can see, the summation equation itself is fairly straightforward, the more difficult part is generating the appropriate values of θ_n and Φ_n to use in the element pattern function. However, careful use of the 3D rotation matrix and its inverse can make the necessary operations reasonably painless.

The next section deals with the structure of the toolbox, outlining the operation of the main function groups.

3. TOOLBOX OVERVIEW

As you have probably already gathered, the 3D rotation matrix plays pivotal role (ha ha) in the array pattern calculations. It will therefore come as no surprise that the matrix forms the backbone of the array description.

There are a number of global variables used in the toolbox but by far the most important is “array_config” . For an N-element array this is a 3x5xN matrix describing the orientation, position, excitation and element type. The matrix is configured as shown below.

Each of the N elements has an entry :

```
L M N  Xoff   Amp
O P Q  Yoff   Pha
R S T  Zoff   Eltype
```

Where :

```
L M N   Xoff
O P Q   Yoff    is the 3D rotation matrix and offset in (meters)
R S T   Zoff
```

Amp	Element amplitude (linear volts)
Pha	Element phase (radians)
Eltype	Element type (integer) 0,1,2…representing which model to use.

As far as the toolbox operation is concerned the functions can be separated broadly into 3 categories :

Geometry Construction -	These functions are used to fill and or modify the array_config matrix, thereby defining the array to be analysed.
Plotting & Visualisation -	These functions operate on the array_config matrix, calling appropriate lower level calculation functions as required.
Element Models -	These are the element pattern functions.

The following sections expand a little further on each category.

3.1 Geometry Construction

The functions provided for this are high and low level. High level functions include those to construct rectangular, circular or cylindrical arrays directly, also rotate and move groups of elements. Low level functions allow modification of the individual element attributes.

The user can of course fill or modify the array_config matrix in any way that is convenient. The main restrictions are that elements are stored sequentially, with no gaps, starting with element 1. This is because the dimension N of the array is used to determine the number of elements in it, there is no separate variable for N.

All elements in a given array must be of the same type due to the way the array patterns are calculated. I.e. the phase centre for the elements is assumed to be the origin of their local axis set. This approximation is valid for elements of the same type in the far-field since it is their relative position that is important. However, the phase centre of 6-turn helix relative to that of a patch would be rather more difficult to establish using this approach.

Finally, the rotation matrix must be a rotation matrix. It has special properties that can be used to check for errors. If **[Trot]** is such a matrix then :

[Trot] is normalised - The squares of the elements in any row or column sum to 1.
[Trot] is orthogonal - The scalar product of any pair of rows or any pair of cols is 0.

Once the basic geometry has been defined the array can be “controlled” by modifying the element amplitude and phase excitations. The element parameters can be changed individually or by using high level functions to apply amplitude and phase tapers across the whole array.

To verify that the correct geometry has been created there are functions to view the geometry in 2D and 3D and to list the array elements in tabular form. The 3D option is useful to check physical orientations, while the 2D option can be zoomed to identify the element numbering and excitations that can be annotated to the geometry.

3.2 Plotting and Visualisation

Once the array geometry has been defined the array patterns can be calculated and plotted in 2D and 3D. The high level commands allow multiple pattern cuts in theta or phi, and are presented in rectangular and polar form on a dB power scale. The patterns can be normalised with respect to the first pattern, normalised on a pattern by pattern basis or plotted as directivity in dBi.

To plot in dBi, the peak directivity must first be calculated using numerical integration over the complete spherical pattern. The step values for the integration can be chosen by the user but obviously must be small enough to resolve the principal features within the pattern.

Lower level commands enable individual pattern cuts to be specified, allowing the user to customise the analysis or make comparisons with measured data.

3.3 Element Models

The element models are mostly taken from standard antenna texts (see references) and represent the far-field element radiation patterns as closed form mathematical solutions (equations).

When patterns are requested, the appropriate values of theta and phi are found in the global coordinate system. Then using orientation and position data from the array_config matrix, the local theta and phi values are calculated for each element. The local values are then used in the element model to find its contribution to the array pattern as a whole.

There are a few things that need to borne in mind when using this approach and possibly easier to list as advantages and disadvantages:

+ Assuming the equation is not too complicated the calculation is potentially very fast.

+ Because the equations have input parameters of element width, height, length dielectric constant etc. Changes to element configurations are very quick and simple.

+ The “tokenised” description of the array geometry means it can be altered very easily.

+ The models take no account of input impedance or bandwidth and assume excitation in the fundamental mode, so you don’t have to worry about tuning the element itself, just the array parameters.

- The models take no account of input impedance or bandwidth and assume excitation in the fundamental mode. The down side of this is of course is that ultimately the element will require tuning to achieve a suitable impedance and bandwidth.

- Elements are limited to those with mathematical models. Arbitrary forms have to be modelled on a full wave solver and element patterns interpolated from a fixed set of calculated data.

- There is no account taken of mutual coupling between the elements. This can have a significant effect on array performance when array elements themselves are large e.g. helices, elements are closely spaced or large scan angles are used.

4. DIRECTIVITY AND POLARISATION

Although the element models used to construct the arrays can be used analytically to find the directivity of an element, calculating closed form solutions for arbitrary arrays of elements is rather more difficult, and best done numerically. The same difficulties arise in resolving polarisation components for an array, in this case a geometry based solution is preferable.

4.1 Directivity

Directivity is defined as the ratio of an antenna's radiation intensity in a given direction over the radiation intensity of an isotropic source (one that radiates equally in all directions). Directivity is often expressed in dBi and represents the dB ratio w.r.t the isotropic radiator, much the same way as dBm is used for rf power. It can be calculated using Eq 4.1-1.

$$D = \frac{U_{\max}}{\frac{1}{4\pi} P_{rad}} \qquad \text{Eq 4.1-1}$$

Where

$U_{\max} = (E_{\max} \cdot E^*_{\max}) =$ Maximum radiation intensity (W / solid angle)

$P_{rad} =$ Total radiated power (W)

The 4π refers to the number of steradians in a sphere, there by giving the denominator units of (W / solid angle) as well. It also means that the denominator represents the average radiation intensity over the sphere.

For a non isotropic antenna (all practical antennas) the total power radiated P_{rad} be found by integrating the radiated power pattern U(θ,Φ) over a full sphere. Substituting this integrated expression for P_{rad} into Eq 4.1-1 gives

$$D = \frac{U_{\max}}{\frac{1}{4\pi} \int_0^{2\pi} \int_0^{\pi} U(\theta, \phi) \cdot \sin(\theta) \cdot d\theta d\phi} \qquad \text{Eq 4.1-2}$$

The numerical equivalent of equation 4.1-2 can be written

$$D = \frac{U_{\max}}{\frac{1}{4\pi} \sum_{j=1}^{M} \left[\sum_{i=1}^{N} P(\theta_i, \phi_j) \cdot \sin(\theta_i) \cdot \Delta\theta\Delta\phi \right]} \qquad \text{Eq 4.1-3}$$

In practice the theta and phi summations use values :

Theta=(start Δθ : step Δθ : stop(π- Δθ)) and Phi=(start ΔΦ : step ΔΦ : stop(2π- ΔΦ))

4.2 Polarisation

All of the element models in this application give the total radiated E-field as a function of their local theta, phi coordinates. In other words there is no polarisation information as such in the element patterns.

However due to the consistent way the element model coordinate systems have been specified, it is possible to resolve the total field patterns into vertical and horizontal components geometrically.

Linearly Polarised Elements

All linearly polarised element models are arranged such that their E-field component is coincident with the X-axis. By representing the X-axis as a unit vector, the vertical and horizontal components of the vector (as viewed by a distant observer), represent directly the vertical and horizontal components of the E-field. Figs 4.2-1a/b show a simple example.

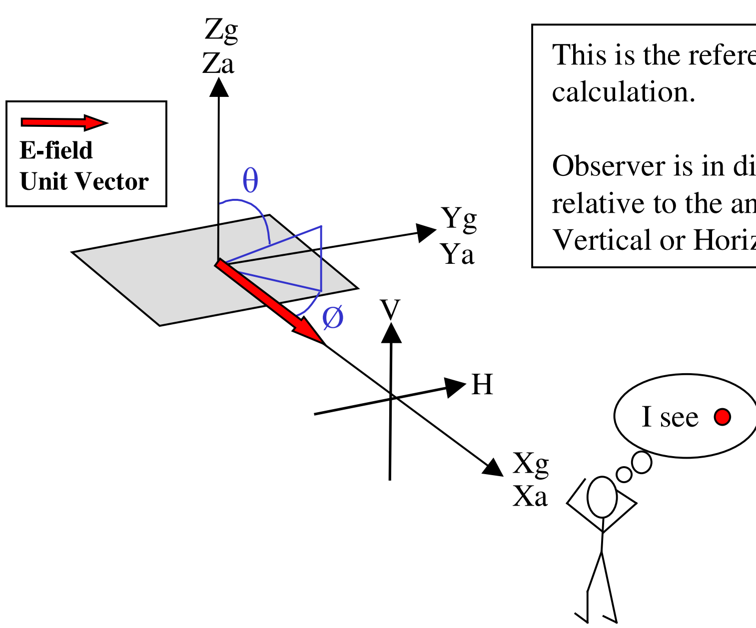

This is the reference for the polarisation calculation.

Observer is in direction (θ=90 , Ø=0) relative to the antenna. He ‘sees’ no Vertical or Horizontal components.

Figure 4.2-1a Polarisation Geometry 1

For example, to resolve the field components for the patch element shown in figure 4.2-1a, in the direction (θ= - 30°,Φ= +0°).

The element is rotated in the opposite sense to point in the direction (θ= + 30°,Φ= +0°), as shown in figure 4.2-1b. The vertical components are given by the Z-axis components of the E-field unit vector. The horizontal components are given by the Y-axis components of the E-field vector.

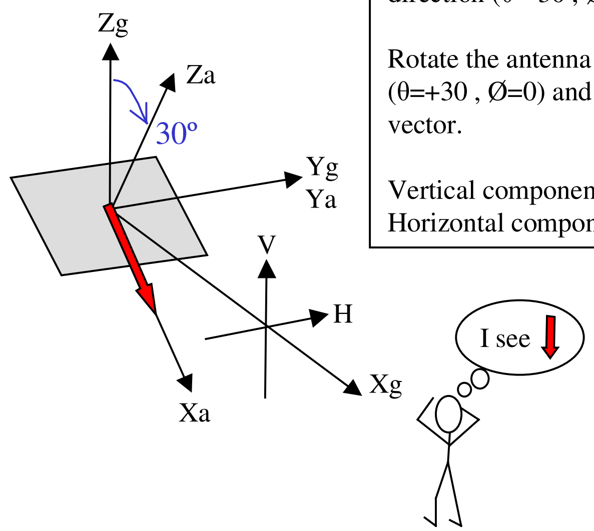

Taking a simple case first, to obtain the polarisation components for a point in the direction (θ=-30 , Ø=0)

Rotate the antenna in the opposite sense to (θ=+30 , Ø=0) and 'look' at the E-field unit vector.

Vertical component would be [-0.5]
Horizontal component would be [0]

Figure 4.2-1b Polarisation Geometry 1

The observer, at some distant point along the X-axis therefore 'sees' the following E-field components.

$E_{vertical} = -0.5$

$E_{horizontal} = 0$

$E_{total} = (|E_{vertical}|^2 + |E_{horizontal}|^2)^{1/2} = 0.5$

In this way the total, vertical and horizontal E-field components are obtained for each element in the array. The polarisation components are summed individually using the array summation equation 2.2-3, giving the separate polarisation components for the array as a whole.The thing to note here that $E_{vertical}$ is negative, the significance of which is illustrated in figure 4.2-2.

In figure 4.2-2 there is a 2-element array that has been constructed by rotate-copy operation on the first element. Looking at the vector components for each element in the direction (θ= +0°,Φ= +0°), so basically as drawn. We see that the E-field vectors are pointing in opposite directions, and therefore have opposite signs for the horizontal vector components. This means as far as the observer is concerned the elements are in anti-phase (assuming the excitation is identical).

Clearly this geometry induced phase reversal must be taken into account, if the correct far-field patterns are to be produced.

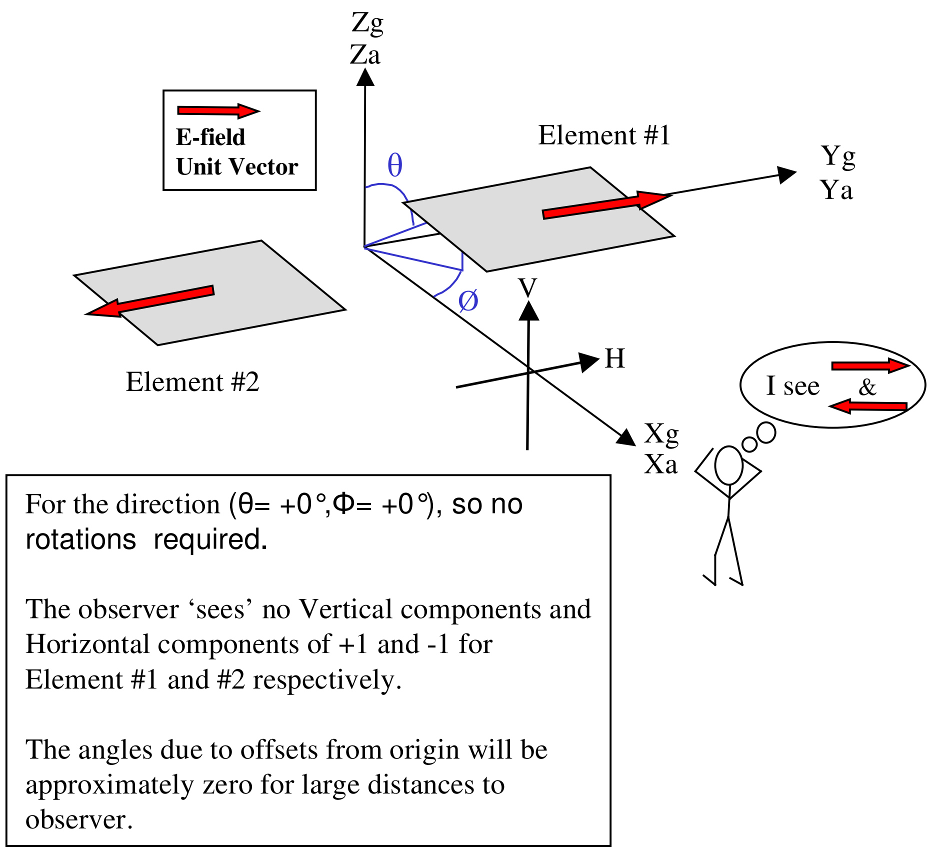

Figure 4.2-2 Polarisation Geometry 2

Fortunately, accounting the phase reversal is just a matter of looking at the sign of the E-field vector component and adding +180° for E^{+ve} and 0° for E^{-ve}. This of course applies to both vertical and horizontal components. Using the far-field summing equation 2.2-3 and including the phase reversal components, we can write the following

$$E_{Vert}(\theta,\phi)=\sum_{n=1}^{N}\vec{E}_{Vert}A_nF_n(\theta_n,\phi_n)e^{-j(ko|r_n|+\beta_n+\gamma_{Vert})} \qquad \text{Eq 4.2-1}$$

$$E_{Horiz}(\theta,\phi)=\sum_{n=1}^{N}\vec{E}_{Horiz}A_nF_n(\theta_n,\phi_n)e^{-j(ko|r_n|+\beta_n+\gamma_{Horiz})} \qquad \text{Eq 4.2-2}$$

$$E_{Total}(\theta,\phi) = \left(\left|E_{Vert}\right|^2 + \left|E_{Horiz}\right|^2 \right)^{1/2}$$ Eq 4.2-3

Where

$\vec{E}_{Vert}$ = Vertical component of E-field unit vector

$\vec{E}_{Horiz}$ = Horizontal component of E-field unit vector

$$\gamma_{Vert} = \left\{ sign(\vec{E}_{Vert}) \cdot (\pi/2) \right\} + (\pi/2)$$

$$\gamma_{Horiz} = \left\{ sign(\vec{E}_{Horiz}) \cdot (\pi/2) \right\} + (\pi/2)$$

The equations Eq 4.2-1 and Eq 4.2-2 give the vertical and horizontal components of the E-field at the far-field point in complex form i.e. Magnitude and phase information. Equation 4.2-3 gives the magnitude of the total field.

Circularly Polarised Elements

The treatment of inherently circularly polarised elements such as the helix is very simplistic, the vertical and horizontal components are just set to the standard polarisation mismatch loss factor (0.7071 or -3.01dB) down on Etotal, for all theta and phi.

Circular polarisation analysis using the resolved vertical and horizontal components has been included for ArrayCalcV2.0 using equations Eq 4.2-1, 4.2-2 and those in Appendix A. Circularly polarised elements can be produced by simply overlaying two linear elements at right angles to each other and exciting them in phase quadrature (90deg with respect to each other). Or by placing elements at right angles to each other, exciting them in-phase, and placing them $\lambda/4$ apart in the direction of propagation.

The diagram in figure 4.2-3 shows circular polarisation using dipoles. However, any linear elements can be used in this way, keeping in mind of course the practicalities. For example method 1 can be used with a patch element to represent the orthogonal modes. While method 2, although possible in ArrayCalc, would be tricky in practice. See [1] for a comprehensive definition of circular polarisation sense.

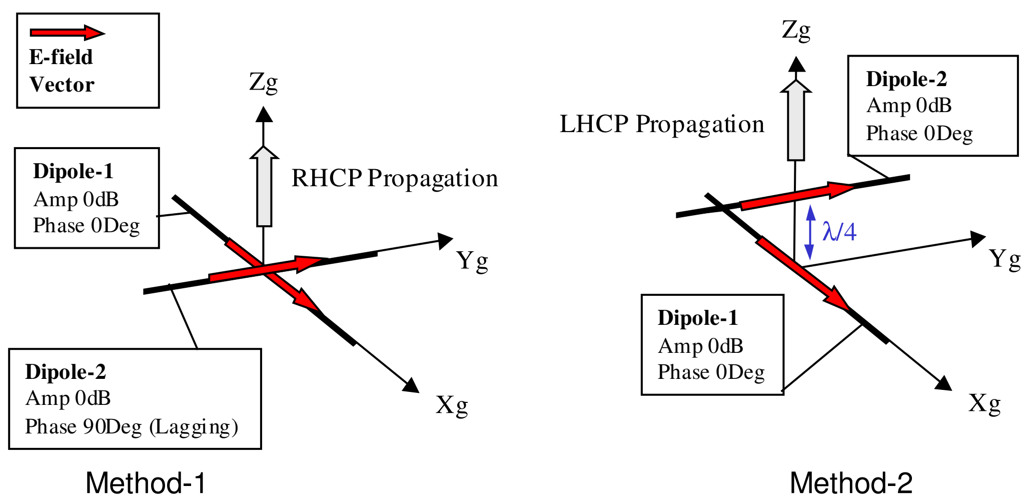

Figure 4.2-3 Circular Polarisation using crossed dipoles

The cautionary note here is that ArrayCalc is only summing idealised E-field vectors. Actually producing highly independent orthogonal polarisations (modes) on anything other than a pair of crossed dipoles is quite hard in practice.

In addition, when an array comprising elements that support a cross-polar component (e.g. patches or crossed-dipoles) is scanned, considerable amounts of cross-polar coupling can be generated, even if only one polarisation (mode) is excited. This effect is due to mutual coupling and will not be modelled by ArrayCalc.

Overall

The polarisation resolving method for has been validated against NEC models and found to be in good agreement for arrays with electrically small elements, exhibiting low mutual coupling. For arrays with large elements and high levels of mutual coupling, as might be found in arrays of long Yagi antennas, the method is less effective. The reasons for this are two-fold: First the origin of the E-field is distributed, so a single unit vector is not a very good representation. Second the mutual coupling causes the array excitation to change, so the contributions from individual elements may not be accurate.

The comments above should be taken special note of when using the ‘interp’ element (ref section 5.11) to array externally generated field patterns of electrically large elements.

5. ELEMENT MATHEMATICAL MODELS

This section describes the mathematical models that are used for the element types included in the toolbox. Generally the models follow those presented in standard antenna texts [1],[2] and [3] except for some minor modifications specific to this application. The modifications principally involve the axis system for the model, roll-off at the pattern edges and side-lobe level adjustment.

The only other difference is that common factors in the standard equations have been removed. These factors represented the propagation constants and excitation voltages/ currents, so actual field strengths could be calculated. In this application the propagation factor and element excitations are part of the array summation, see Eq2.2-3

5.1 Helix

The model for the helix antenna treats the helix as an array of loops, each with identical current distribution and phase separation with respect to each other. The diagram in figure 5.1-1 shows the principal dimensions.

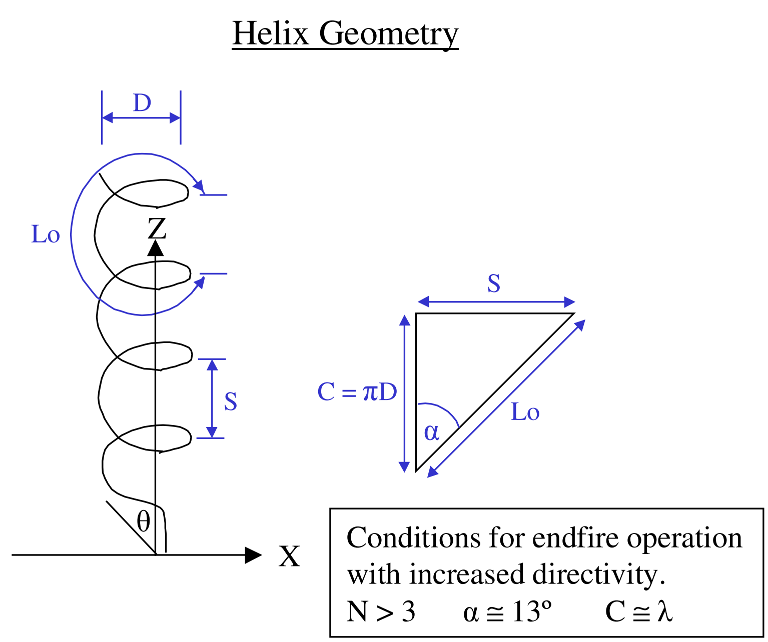

Figure 5.1-1 Helix Geometry

There are various possible operating modes for the helix, determined by its electrical dimensions at the frequency of operation, [2] is a good source of additional information. For this application the helix is assumed to be operating in the end-fire, increased directivity (or Hansen-Woodyard) condition. This is in fact the most common use of the helix antenna.

The Hansen-Woodyard condition refers to the phase change between loops of the helix. For ordinary end-fire operation, the loops would be phased according to their physical position. For example if the loop spacing in an N element array represented 90° in free space, then each loop would be phased -90° from its neighbour, in the direction of propagation. Hansen and Woodyard discovered that if the same array had elements phased -(90°+180°/N) with respect to each other, the array had significantly improved directivity. Not only this, but also certain helix geometries naturally hold this mode over a wide bandwidth, an octave or more.

The equation 5.1-1 below is the standard formulation the radiation pattern of an N-turn helix, operating in the increased directivity condition, Etotal is in linear volts.

$$Etotal = \sin\left(\frac{\pi}{2N}\right)\cos(\theta)\frac{\sin[(N/2)\psi]}{\sin[\psi/2]} \qquad \text{Eq 5.1-1}$$

Where :

$$\psi = ko\left(S\cos(\theta) - \frac{Lo}{p}\right) \qquad \textbf{or} \qquad \psi = ko\left(S(\cos(\theta - 1) - \lambda o\left(\frac{2N+1}{2N}\right)\right)$$

$$p = \frac{Lo/\lambda o}{S/\lambda o + \left(\frac{2N+1}{2N}\right)} \qquad \text{Indicating no dependence on Lo}$$

$$ko = 2\pi/\lambda o$$

The equation is a little misleading in that it implies that it is dependent on the turn length Lo. With a little algebra it is possible to show that this is not the case, because Lo is fixed by the value of the turn spacing S and pitch angle alpha (see the alternative formulation for psi in Eq5.1-1). The values of alpha and circumference C are constrained to approximately 13deg and 1λ respectively by the need for the increased directivity condition. This is the reason why the helix configuration parameters in the global variable helix_config are limited to N and S. In the actual MATLAB code, values for C and Lo are calculated from S and used in the standard form to make the equations look more familiar.

During initial validation of the equation model, patterns were compared with a NEC2 model and found to be in good agreement for the main lobe parameters. However the side-lobe levels given by the model were significantly lower than those from the NEC2 implementation or indeed that could be realistically expected from a practical design. This is because the equation model assumes perfect current and phase distributions along the helix. While the approximation is good for very long helicies, shorter helicies can deviate significantly from the ideal.

To compensate for this shortcoming, the standard helix pattern Eq 5.1-1 is multiplied by a pattern scaling function Eq 5.1-2 to raise the side-lobe levels in proportion to theta squared, giving the helix far-field pattern Eq 5.1-3.

$$PatternSF = \frac{\theta^2}{\pi^2}\left(10^{SSF/20} - 1\right) + 1$$ Eq 5.1-2

Where : SSF is the side-lobe scaling factor in dB (SSF=15 in the model)

PatternSF is equal to the SSF (in linear form) at theta=pi and tends towards 1, as theta tends towards 0.

Although the use of a pattern scaling function may seem a little arbitrary, the intention is simply to make the model slightly closer to reality. To this end, the function works well and for very little extra complexity.

The far-field pattern for the helix is therefore given by :

$$Ehelix = Etotal \cdot PatternSF$$ Eq 5.1-3

5.2 Rectangular Microstrip Patch

The model used for the rectangular microstrip patch is the cavity / transmission-line model and is referenced by most antenna texts covering microstrip antennas. The patch is modelled as 2 radiating slots, separated by a nominally half wavelength section of low impedance transmission line.

The geometry for the patch is shown in figure 5.2-1 and the principal thing to note is the transposition of axes between the local element system (used in the array calculations) and the system as defined in the model. The main patch parameters are :

- Length of the transmission line between the slots L.
- Width of the patch W.
- Patch height h.

The E-theta and E-phi components of the far-field radiation patterns are given by Eq 5.2-1 and Eq5.2-2 respectively.

$$E_\theta total = \left\{ \sin(\theta) \frac{\sin\left(\frac{ko \cdot h}{2}\sin(\theta)\right)}{\frac{ko \cdot h}{2}\sin(\theta)} \frac{\sin\left(\frac{ko \cdot W}{2}\cos(\theta)\right)}{\frac{ko \cdot W}{2}\cos(\theta)} \right\}$$ Eq 5.2-1

$$E_\phi total = \left\{ \frac{\sin\left(\frac{ko \cdot h}{2}\cos(\phi)\right)}{\frac{ko \cdot h}{2}\cos(\phi)} \right\} \cos\left(\frac{ko \cdot Le}{2}\sin(\phi)\right)$$ Eq 5.2-2

Where :

$$ko = 2\pi / \lambda o$$

$$Le = L + 2 \cdot \Delta L$$ The patch looks longer electrically due to the fringing fields at each end.

$$\Delta L = h(0.412)\frac{(Er_{eff} + 0.3)\left(\frac{W}{h} + 0.264\right)}{(Er_{eff} - 0.258)\left(\frac{W}{h} + 0.8\right)}$$ Increase in length at each end of the patch.

$$Er_{eff} = \frac{Er + 1}{2} + \frac{Er - 1}{2}\left[1 + 12\frac{h}{W}\right]^{-1/2}$$

Modification of Er to account for fringing fields at the sides of the microstrip (Valid for W/h >1)

Rectangular Patch Geometry

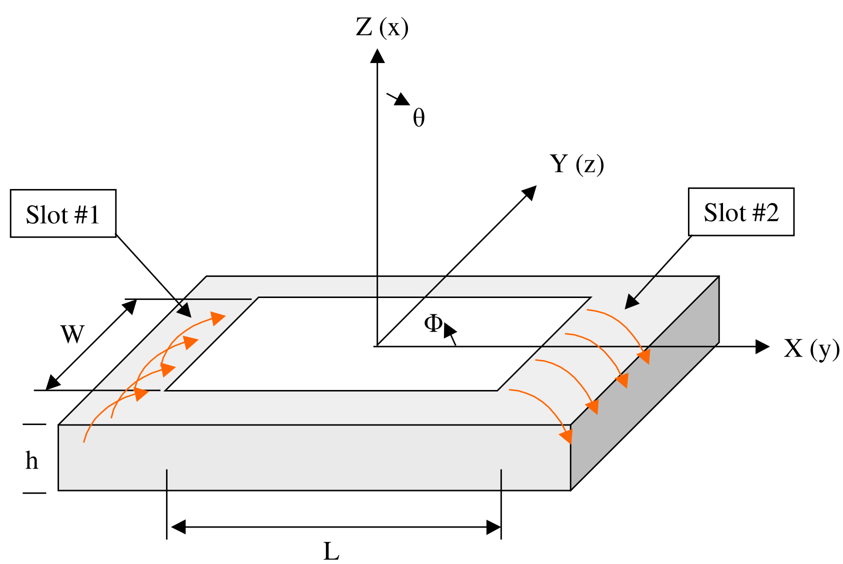

Co-ordinate Axis Transposition

X,Y,Z is the local element coordinate system used for the array calculation. Theta and Phi are the spherical coordinate directions.

(x),(y),(z) is the co-ordinate system as defined in the model. Theta and Phi in the model are defined in the same sense except w.r.t. (x),(y) and (z).

Figure 5.2-1 Rectangular Patch Geometry

Elements using ground planes such as patches and helicies have models that assume infinite ground planes and are therefore only valid over the hemisphere 0°<theta<90°, 0°<phi<360°. Also, since it is possible to define conformal arrays it is highly likely that the local (theta, phi) values will lie outside the valid range for some of the elements, for a given far-field pattern.

For helicies it is simply a matter of defining the pattern (in linear volts) to be zero for theta>90deg. For patches the cavity model is used and things are slightly more complicated. The cavity model in the E-plane is fairly accurate for theta values less than 70deg. However, beyond 70deg the roll-off exhibited by more accurate models and measured examples is not reproduced. Instead the pattern truncates at theta=90deg, at around –8dB down on maximum, depending on the patch design. Leaving this step in the pattern would severely limit the analysis of conformal arrays, see figures 5.2-2a/b.

To alleviate the problem a roll-off can be applied as a pattern scaling factor (PatternSF) using a simple function of the local theta value (in degrees), and is of the form :

$$PatternSF = \frac{1}{\dfrac{1}{(RollOff\,(\theta - 90))^2 + K} + 1} \qquad \text{Eq 5.2-3}$$

RollOff is the roll-off factor between 0 and 1 (1=sharp 0=soft), typical value 0.15

K is a small offset to avoid infinities at theta=90, typical value 0.001

The total far-field pattern for the rectangular patch is therefore given by the following equation :

$$Epatchr = E_\phi total \cdot E_\theta total \cdot PatternSF \qquad \text{Eq 5.2-4}$$

The justification for this modification of the standard model is that for this application it gives more accurate results when looking at conformal arrays or theta values approaching 90 degrees.

The geometry and patterns in Figures 5.2-2a/b illustrate the roll-off problem. The geometry represents 2 rectangular patches 0.7 lambda apart and rotated –30deg and +30deg respectively about the global Y-axis.

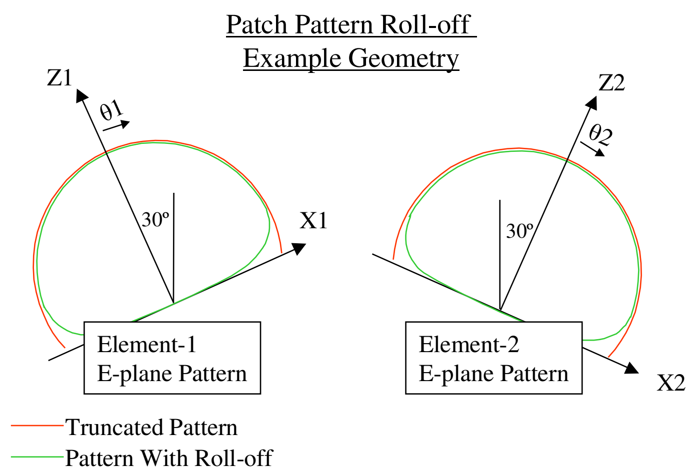

Figure 5.2-2a 2-element array geometry

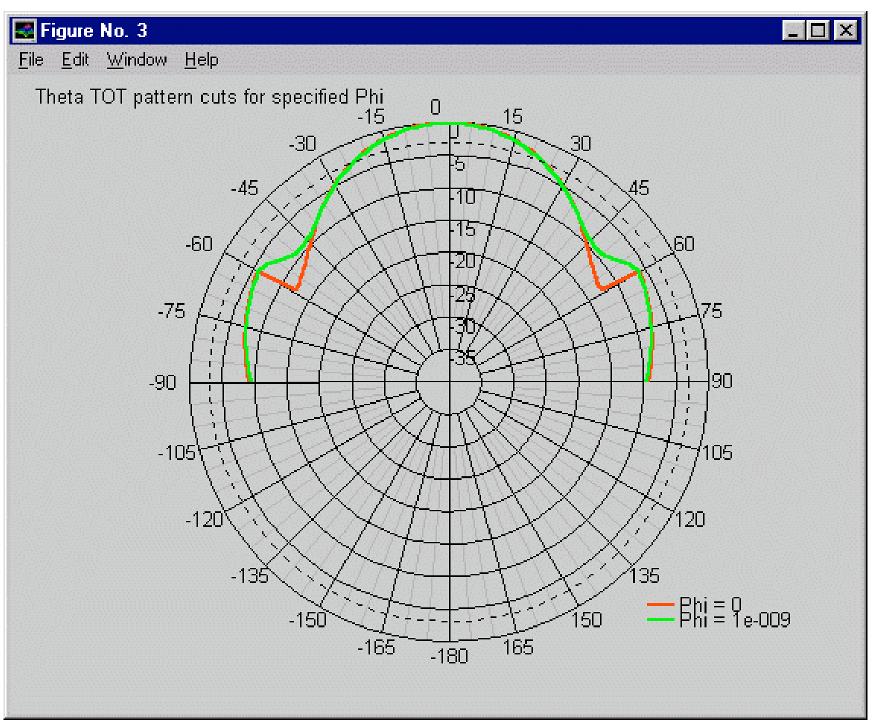

Figure 5.2-2b 2-element array with/wout roll-off

The calculated patterns with and without roll-off clearly show the discontinuities in the calculated far-field pattern if no roll-off is used. While this may seem a little obvious and trivial for a 2 element array, for large arrays with complex patterns it is not.

5.3 Circular Microstrip Patch

The circular microstrip patch uses the cavity model, simplified to a circular loop for large values of a/h (see figure 5.3-1). The operation of a circular patch in the fundamental mode TM^{z}_{110} is pretty much the same as for the rectangular patch except the dimensions are determined solely by the radius a.

The far-field radiation patterns are calculated using the following equations :

$$E_{\theta} = -j(\cos(\phi) Ja_{02})F \qquad \text{Eq 5.3-1}$$

$$E_{\phi} = +j(\cos(\theta)\sin(\phi) Jb_{02})F \qquad \text{Eq 5.3-2}$$

Where :

$$Ja_{02} = J_0(ko \cdot a_e \cdot \sin(\theta)) - J_2(ko \cdot a_e \cdot \sin(\theta))$$

$$Jb_{02} = J_0(ko \cdot a_e \cdot \sin(\theta)) + J_2(ko \cdot a_e \cdot \sin(\theta))$$

$$F = \frac{\sin(ko \cdot h \cdot \cos(\theta))}{ko \cdot h \cdot \cos(\theta)}$$ For completeness, but generally close to unity for small h.

$$ko = 2\pi / \lambda o$$

$$a_e = a\left\{1 + \frac{2h}{\pi \cdot a \cdot Er}\left[\ln\left(\frac{\pi a}{2h}\right) + 1.7726\right]\right\}^{1/2}$$ Effective radius due to fringing fields.

J_0 denotes zero order Bessel function of the first kind.

J_2 denotes second order Bessel function of the first kind.

The total far-field pattern for the circular patch is given by the following equation :

$$Epatchc = \left(\left|E_{\theta}\right|^2 + \left|E_{\phi}\right|^2\right)^{1/2} \cdot PatternSF$$

Etheta and Ephi are Eq 5.3-1 and 5.3-2 respectively

PatternSF is given by Eq 5.2-3 and reasons for its use are covered in section 5.2

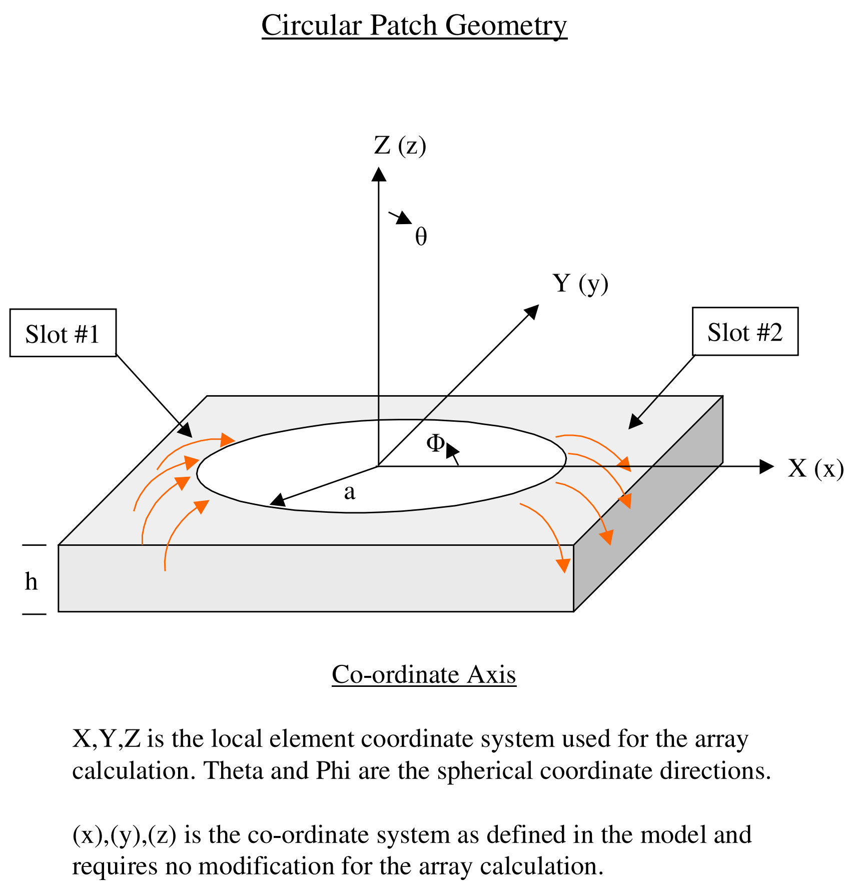

Figure 5.3-1 Circular Patch Geometry

Generally the circular patch has slightly inferior performance to its rectangular cousin, its efficiency and bandwidth being lower. There is however less copper area for a given resonant frequency, this maybe beneficial in terms of mutual coupling.

5.4 Dipole

The dipole model is again standard issue in most antenna texts and is derived by integrating the field contributions from a line of infinitesimal dipole elements.

The model used here is for an arbitrary dipole of finite length and as such need not be λ/2, although this is by far the most common usage. The model assumes a sinusoidal current distribution symmetrical about a central feed point. If you are tempted to experiment with lengths other than usual λ/2, it might be wise to investigate the implications regarding input impedance first.

The field pattern and geometry for the dipole are given be Eq 5.4-1 and figure 5.4-1 respectively.

The equation for the dipole far-field pattern is as follows :

$$Edipole = \left\{ \frac{\cos\left(\frac{ko \cdot l}{2}\cos(\theta)\right) - \cos\left(\frac{ko \cdot l}{2}\right)}{\sin(\theta)} \right\} \qquad \text{Eq 5.4-1}$$

Where

$ko = 2\pi / \lambda o$

$l =$ Dipole length (m)

Dipole Geometry

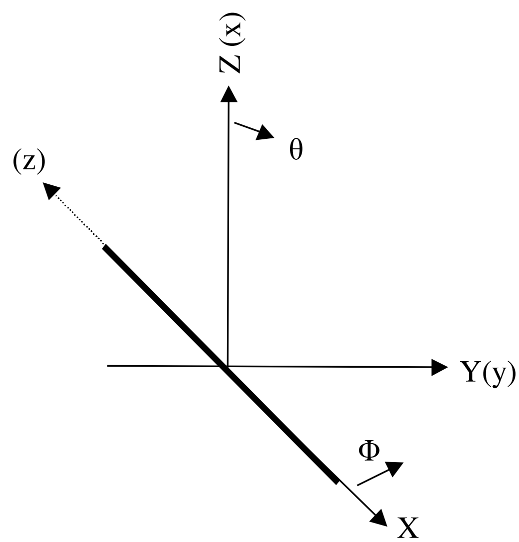

Co-ordinate Axis Rotation

X,Y,Z is the local element coordinate system used for the array calculation. Theta and Phi are the spherical coordinate directions. X,Y,Z are (x),(y),(z) rotated -90deg around the common Y(y)-axis

(x),(y),(z) is the co-ordinate system as defined in the model. Theta and Phi in the model are defined in the same sense except w.r.t. (x),(y) and (z).

Figure 5.4-1 Dipole coordinate geometry

5.5 Dipole over ground

The dipole over a ground plane model is the same as for the normal dipole except that it is used twice. For a dipole placed at height h above a plane, a second 'image' dipole is placed at –h below the plane and phased at 180deg w.r.t. the first, creating a virtual ground plane between the two. An intermediate array calculation is performed on the dipoles to generate a far-field pattern for the pair.

The field pattern and geometry for the dipole are given be Eq 5.5-1 and figure 5.5-1 respectively.

$$Edipoleg_{(R,\theta,\phi)} = \left| Edipole1 \cdot (e^{-j(ko \cdot r1)}) + Edipole2 \cdot (e^{-j(ko \cdot r2 - \pi)}) \right| \qquad \text{Eq 5.5-1}$$

Where

$$Edipole1 = \left\{ \frac{\cos\left(\frac{ko \cdot l}{2}\cos(\theta_1)\right) - \cos\left(\frac{ko \cdot l}{2}\right)}{\sin(\theta_1)} \right\}$$

$$Edipole2 = \left\{ \frac{\cos\left(\frac{ko \cdot l}{2}\cos(\theta_2)\right) - \cos\left(\frac{ko \cdot l}{2}\right)}{\sin(\theta_2)} \right\}$$

$ko = 2\pi / \lambda o$

$l =$ Dipole length (m)

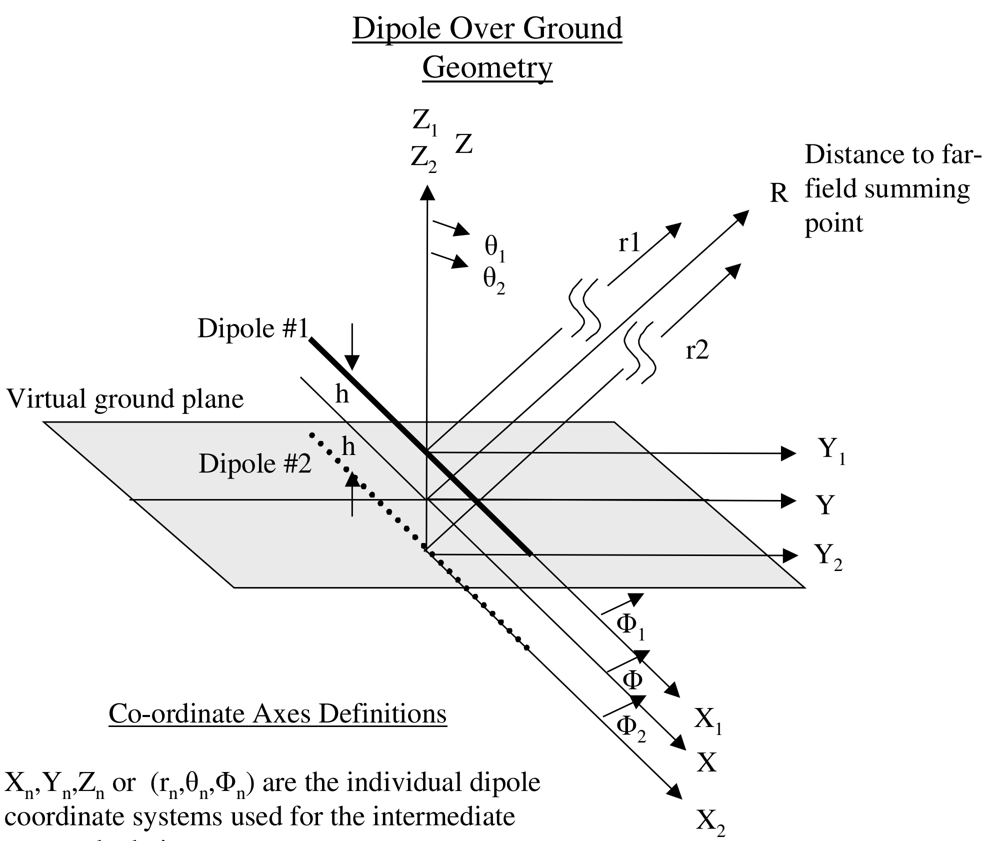

X_n,Y_n,Z_n or (r_n,θ_n,Φ_n) are the individual dipole coordinate systems used for the intermediate array calculation.

X,Y,Z or (R,θ,Φ) is the axis system for the dipole pair in the main array calculataion.

The only additional point I would make here is that although the dipole looks very simple to implement at the modelling stage, bear in mind that each one will ultimately require a balun of some description, which can add considerably to the cost in a high volume application.

5.6 Rectangular Aperture

The rectangular aperture model is for a rectangular, uniform E-field distribution within an infinite groundplane. The orientation and dimensions of the aperture are shown in figure 5.6-1 below.

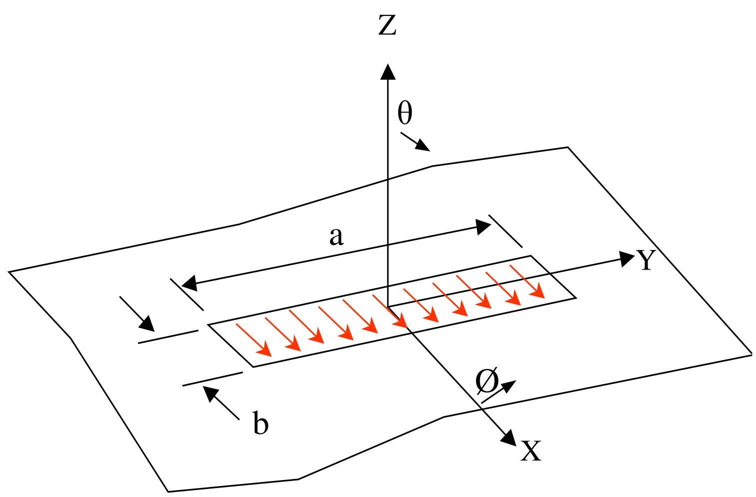

Figure 5.6-1 Rectangular Aperture Configuration

$$E_\theta = \sin(\phi)\cdot\frac{\sin X}{X}\cdot\frac{\sin Y}{Y}$$ Eq 5.6-1

$$E_\phi = \cos(\theta)\cdot\cos(\phi)\cdot\frac{\sin X}{X}\cdot\frac{\sin Y}{Y}$$ Eq 5.6-2

Where :

$$X = \frac{ka}{2}\cdot\sin(\theta)\cdot\sin(\phi)$$

$$Y = \frac{kb}{2}\cdot\sin(\theta)\cdot\cos(\phi)$$

$$k = \frac{2\pi}{\lambda}$$ *Propagation factor*

5.7 Rectangular Waveguide Aperture

The rectangular waveguide aperture model is for an open-ended rectangular waveguide supporting the TE_{10} mode. The orientation and dimensions of the aperture are shown in figure 5.7-1 below.

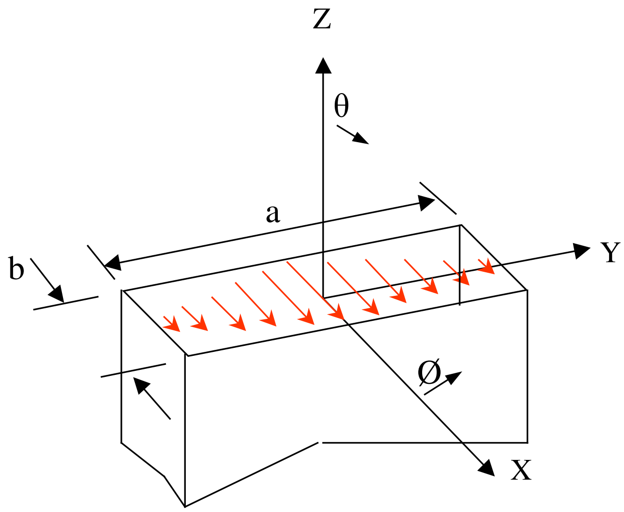

Figure 5.7-1 Rectangular Waveguide Configuration

$$E_\theta = \sin(\phi)\cdot\frac{\cos X}{X^2-\left(\frac{\pi}{2}\right)^2}\cdot\frac{\sin Y}{Y} \qquad \text{Eq 5.7-1}$$

$$E_\phi = \cos(\theta)\cdot\cos(\phi)\cdot\frac{\cos X}{X^2-\left(\frac{\pi}{2}\right)^2}\cdot\frac{\sin Y}{Y} \qquad \text{Eq 5.7-2}$$

Where :

$$X = \frac{ka}{2}\cdot\sin(\theta)\cdot\sin(\phi)$$

$$Y = \frac{kb}{2}\cdot\sin(\theta)\cdot\cos(\phi)$$

$$k = \frac{2\pi}{\lambda}$$ *Propagation factor*

5.8 Circular Aperture

The circular aperture model is for a circular, uniform E-field distribution within an infinite groundplane. The orientation and dimensions of the aperture are shown in figure 5.8-1 below.

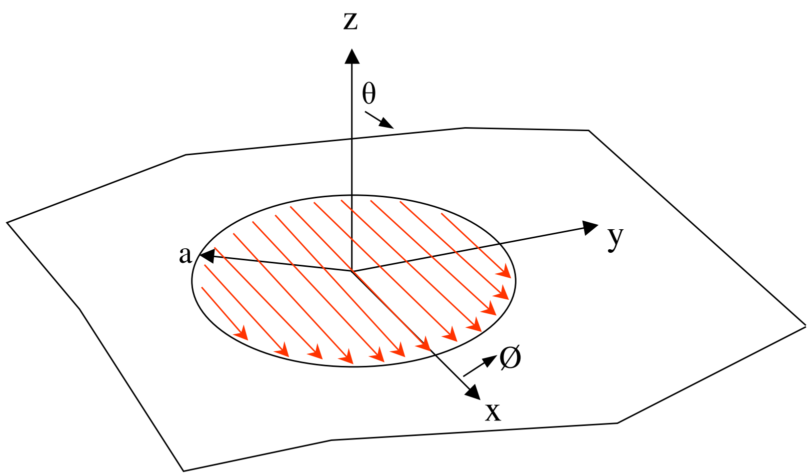

Figure 5.8-1 Circular Aperture Configuration

$$E_\theta = \cos(\phi) \cdot \frac{J_1(Z)}{Z} \quad \text{Eq 5.8-1}$$

$$E_\phi = \cos(\theta) \cdot \sin(\phi) \cdot \frac{J_1(Z)}{Z} \quad \text{Eq 5.8-2}$$

Where :

$Z = ka \cdot \sin(\theta)$ *(a is the aperture radius)*

$k = \frac{2\pi}{\lambda}$ *Propagation factor*

5.9 Circular Waveguide Aperture

The circular waveguide aperture model is for an open-ended circular waveguide supporting the TE_{11} mode. The orientation and dimensions of the aperture are shown in figure 5.9-1 below.

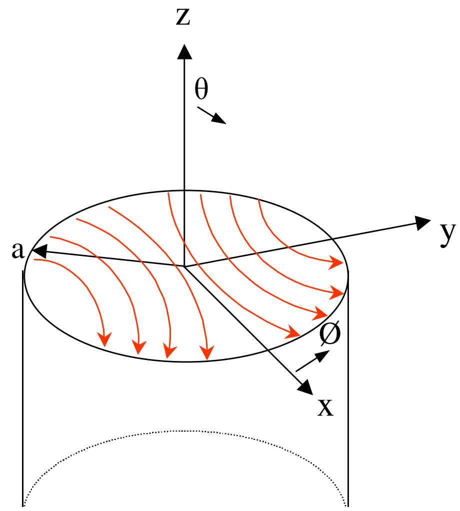

Figure 5.9-1 Circular Waveguide Aperture Configuration

$$E_\theta = \cos(\phi)\cdot\frac{J_1(Z)}{Z}$$ Eq 5.9-1

$$E_\phi = \cos(\theta)\cdot\sin(\phi)\cdot\frac{J_1(Z)}{1-(Z/\chi_{11})^2}$$ Eq 5.9-2

Where :

$Z = ka\cdot\sin(\theta)$ *(a is the aperture radius)*

$\chi_{11} = 1.841$

$k = \dfrac{2\pi}{\lambda}$ *Propagation factor*

5.10 Parabolic Dish Aperture

The circular parabolic dish aperture is represented by a linearly polarised aperture field with an amplitude taper as a function of radial distance (ρ) to the edge of the dish (a).

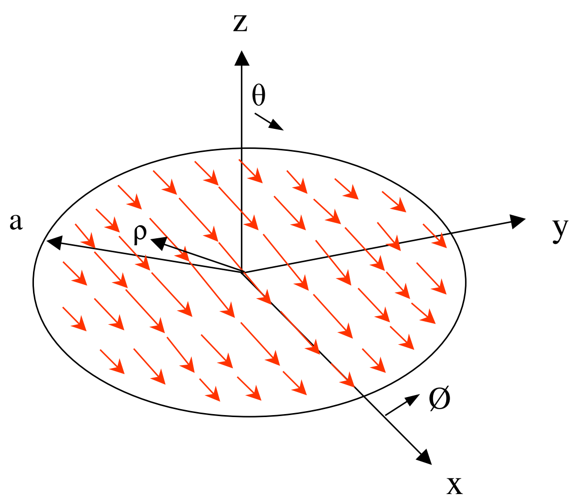

Figure 5.10-1 Parabolic Dish Aperture Configuration

The amplitude taper is described by

$$\left|\vec{E}\right| = \left[(1-A) + A\left(1-\frac{\rho^2}{a^2}\right)^n\right]$$ magnitude of aperture E-field Eq 5.10-1

Where

a = Edge of aperture radius

ρ = Radial distance from aperture centre

A = Linear value of aperture field at aperture edge A(dB)=20*log10(A)

n = Amplitude taper factor, rate at which the amplitude drops to value A

An amplitude taper of 10.5dB (A=0.3) provides optimum gain. Increasing the taper will reduce sidelobe levels further, at the expense of gain.

The factor n effectively describes how the feed illuminates the dish, higher gain feeds will have a higher n-value, a typical value for n is around 2.5.

The Etheta and Ephi patterns are given by

$$E_{\theta} = \cos(\phi)\cdot Z \qquad \text{Eq 5.10-2}$$

$$E_{\phi} = \cos(\theta)\cdot\sin(\phi)\cdot Z \qquad \text{Eq 5.10-3}$$

Where

$$Z = \left[2(1-A)\frac{J_1(u)}{u} + A\cdot 2^n \cdot (n+1)!\cdot\frac{J_{n+1}(u)}{u^{n+1}} \right]$$

$$u = ka\cdot\sin(\theta)$$

$$k = \frac{2\pi}{\lambda}$$ *Propagation factor*

5.11 Interpolated

There are obviously going to be occasions when the built in models are not applicable, the 'interp' element provides a means of arraying elements defined by a set of pattern cuts from an external source. These may be measured data or data calculated using a more suitable package.

The basic operation of the routine is illustrated in the flow chart 5.11-1

Interpolated Data Element
Flow Chart

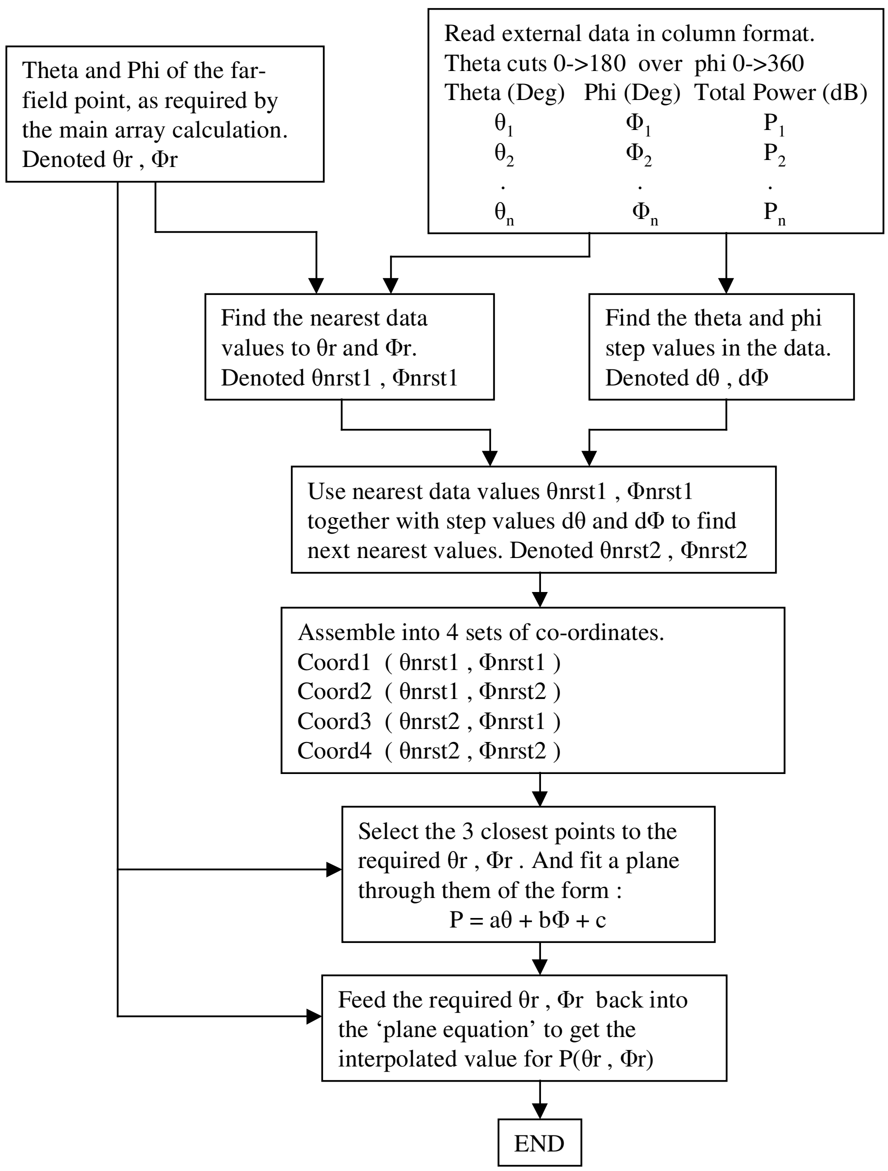

Figure 5.11-1 Interpolation Flowchart

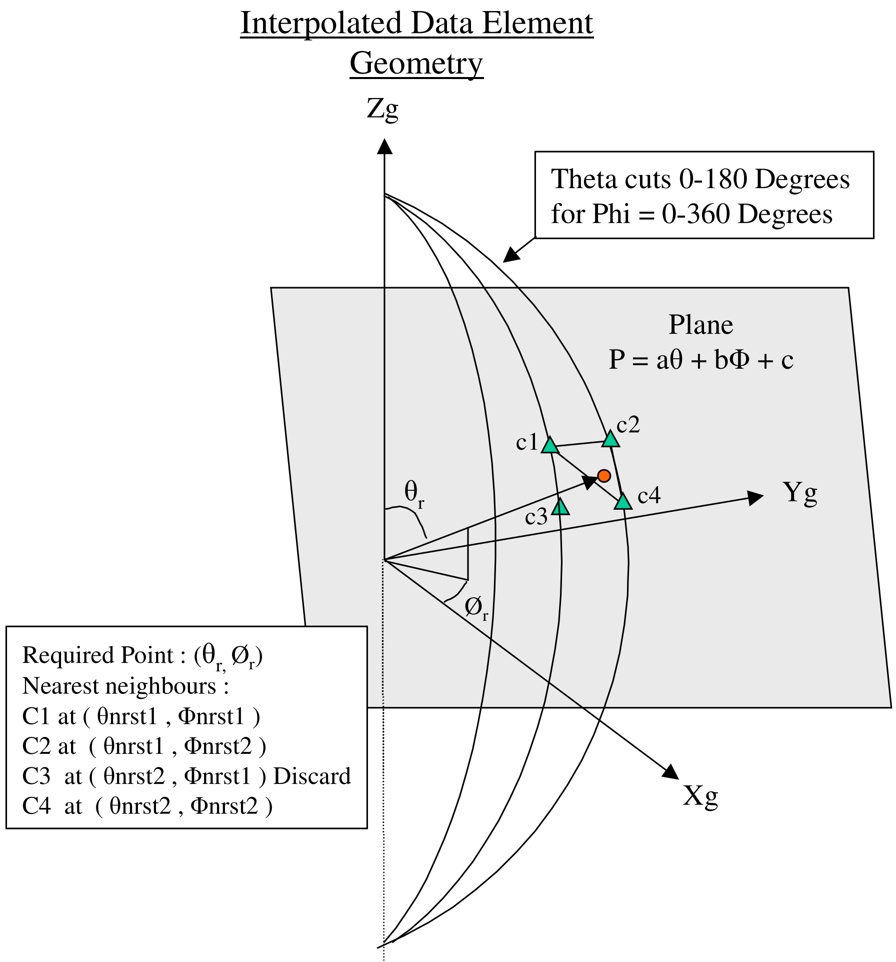

Figure 5.11-2 Interpolation Geometry

Hopefully the algorithm description will allow the user to trouble-shoot any problems using this function. The main requirements are that the data complies with the following :

- Theta cuts from 0 to 180 degrees for Phi values from 0 to 360, step values should be even. A full sphere data set is required to calculate directivity.
- Theta and Phi values should be in ascending order.
- Ideally the direction of propagation for the element is the Z-axis. For linearly polarised elements the E-field should be aligned with the X-axis, for consistency with other element models.

If a full sphere data set is not available then it should still be possible to plot normalised pattern data. For example element data for (0<theta<90, 0<phi<360) is sufficient for a planar array.

7. REFERENCES

[1] "Antenna Theory Analysis and Design" 2nd edition by Constantine A. Balanis. Published Wiley ISBN 0-471-59268-4

[2] "Antennas" 2nd edition by John D. Kraus. Published McGraw-Hill ISBN 0-07-100482-3

[3] "Antenna Engineering Handbook" 1st edition edited by Henry Jasik. Published McGraw-Hill

[4] "Microstrip Antennas" by I.J. Bahl and P. Bartia. Published Artech House ISBN 0-89006-098-3

[5] "Numerical Recipes in C" 2nd edition by William H. Press, Saul A. Teukolsky, William T. Vetterling, Brian P. Flannery. Published Cambridge University Press ISBN 0-521-43108-5

[6] "MATLAB User Guide" The Math Works

APPENDIX A

Equations for use in the analysis of circular polarisation, see file : fieldsum.m.

$$E_{MAJOR} = \left[\frac{1}{2} \left\{ E_{HP}^2 + E_{VP}^2 + \left[E_{HP}^4 + E_{VP}^4 + 2 \cdot E_{HP}^2 E_{VP}^2 \cdot \cos(2\Delta\gamma) \right]^{1/2} \right\} \right]^{1/2} \quad \text{Eq A-1}$$

$$E_{MINOR} = \left[\frac{1}{2} \left\{ E_{HP}^2 + E_{VP}^2 - \left[E_{HP}^4 + E_{VP}^4 + 2 \cdot E_{HP}^2 E_{VP}^2 \cdot \cos(2\Delta\gamma) \right]^{1/2} \right\} \right]^{1/2} \quad \text{Eq A-2}$$

$$\tau = \frac{\pi}{2} - \frac{1}{2} \tan^{-1} \left[\frac{2 E_{HP} E_{VP}}{E_{HP}^2 - E_{VP}^2} \cos(\Delta\gamma) \right] \quad \text{Eq A-3}$$

Let angle_diff = (angle($\mathbf{E}_{VP}$)-angle($\mathbf{E}_{HP}$))

If (angle_diff > π or angle_diff < -π) then angle_diff = (π - angle_diff)

For a predominantly left-handed wave : angle_diff is –ve and

$$E_L = \frac{E_{MAJOR} + E_{MINOR}}{\sqrt{2}} \qquad E_R = \left(\frac{E_{MAJOR} - E_{MINOR}}{\sqrt{2}} \right) e^{j \cdot 2 \cdot \tau} \quad \text{Eq A-4a/b}$$

For a predominantly right-handed wave : angle_diff is +ve and

$$E_L = \frac{E_{MAJOR} - E_{MINOR}}{\sqrt{2}} \qquad E_R = \left(\frac{E_{MAJOR} + E_{MINOR}}{\sqrt{2}} \right) e^{j \cdot 2 \cdot \tau} \quad \text{Eq A-5a/b}$$

Where :

E_{MAJOR} and E_{MAJOR} are the major and minor axis of the polarisation ellipse (linear volts).

E_{VP} and E_{HP} are the magnitude of vertical and horizontal E-field components (linear volts).

$\mathbf{E}_{VP}$ and $\mathbf{E}_{HP}$ are vertical and horiz E-field vector components in complex form (linear volts).

γ is the phase angle between $\mathbf{E}_{VP}$ and $\mathbf{E}_{HP}$. τ is the tilt of the polarisation ellipse.

E_L and E_R are the magnitudes of left and right hand circularly polarised wave components.

In Eq A-4a/b E_L = LHCP(co-polar) and E_R = LHCP(x-polar)

In Eq A-5a/b E_R = RHCP(co-polar) and E_L = RHCP(x-polar)